

GLOBAL POSITIONING SYSTEM IN CURVED SPACE-TIME
AND OTHER
APPLICATIONS OF GENERAL RELATIVITY

A Dissertation

Submitted to the Graduate Faculty of the
Louisiana State University and
Agricultural and Mechanical College
in partial fulfillment of the
requirements for the degree of
Doctor of Philosophy

in

The Department of Physics and Astronomy

by
Argenis Daniel Da Silva
Licenciado en Física, Universidad de Oriente, Venezuela, 1999
December 2009

Table of Contents

List of Tables	iv
List of Figures	vi
Abstract	vii
Chapter 1. Introduction	1
Chapter 2. The Atmospheric Corrections in GPS	5
2.1 Two Colours Laser Ranging	5
Chapter 3. The Global Positioning System	7
3.1 Description of the System	7
3.2 The Propagation Delay Equations	7
3.3 Relativistic Effects on Clocks	8
3.3.1 Special Relativistic Effects	9
3.3.2 Gravitational Effects	10
3.3.2.1 The Redshift	10
3.3.2.2 The Curvature Delay	10
3.3.2.3 Shapiro Delay	11
3.3.2.4 The Eccentricity Effect	11
3.3.2.5 The Crosslink Ranging	11
Chapter 4. Fully Relativistic Description of the GPS	12
4.1 The Line Element	12
4.2 Examples of the Line Element	13
4.2.1 The Schwarzschild Line Element	13
4.2.2 The Kerr Line Element	14
4.2.3 Line Element for an Oblate Earth	14
4.3 Coordinates in Curved Space-Time	15
4.3.1 Examples of Coordinates in Curved Space-Time	15
4.4 The Proper Time and the Coordinate Time	16
4.5 The Equation of the Geodesics	16
4.6 The Satellite Orbits	17
4.7 The Photons' Trajectory	17
Chapter 5. A Numerical Way Around the Flat Space-Time Delay Equations in GPS	18
5.1 The Motivation	18
5.2 Sending the Initial Conditions	19
5.3 Positioning in Curved Space-time	19
5.4 An Example	21

Chapter 6. Evolution of Anisotropic Stars23
6.1 The Energy-momentum Tensor23
6.2 The Effective Variables24
6.3 The Interior Line Element in Schwarzschild Coordinates24
6.4 The Exterior Line Element25
6.5 The Explicit Form for U^μ and S^μ25
6.6 The Einstein Field Equations26
6.7 The Junction Conditions27
6.8 The Method of the Effective Variables28
6.9 The Equations at the Surface ($r=a(t)$)29
6.10 A Model30
6.11 The Evolution31
Chapter 7. The Klein-Gordon Field36
7.1 The Stress Tensor for the Klein-Gordon Field36
7.2 The Klein-Gordon Equation36
7.3 The Metric36
7.4 The Field Equations37
7.5 Numerical Implementation38
7.5.1 Numerical Grid38
7.5.2 Evolution Equations38
7.5.3 Scattering of Massless Scalar Field39
Bibliography42
Appendix: Permission to Use Copyrighted Material43
Vita44

List of Tables

3.1 Relativistic Effects in GPS8
---------------------------------------	----

List of Figures

2.1	The optical and geometrical distances	.5
2.2	The optical paths for the two-colors laser	.6
3.1	Moving reference frames	.9
4.1	Two observer moving along different paths	.13
4.2	Surfaces $\theta = \text{constant}$ for a flat geometry (left) and for the Schwarzschild geometry (right)	.15
4.3	Difference, in meters, between the radial spherical coordinate and the radial Schwarzschild coordinate for a typical GPS satellite	.16
5.1	The wavefront for the signals	.20
5.2	Numerical reconstruction of the wavefronts, all the distances are expressed in meters	.21
5.3	Search for the closest point to the wavefronts, all the distances are expressed in meters	.22
6.1	Evolution of ω for $h=1.34$.31
6.2	Evolution of the radius for $h=1.34$.32
6.3	Evolution of ω for $h=1.54$.32
6.4	Evolution of the radius for $h=1.54$.33
6.5	Evolution of ω for $h=1.74$.33
6.6	Evolution of the radius $h=1.74$.34
6.7	Evolution of ω for $h=1.74, m(0)=9.9$.34
6.8	Evolution of the radius for $h=1.74, m(0)=9.9$.35
7.1	Axisymmetric surface plots of $r\phi$ for time $u=1, 2, 3, 4$. The parameters of the initial data are $r_a = 3, r_b = 5, \lambda = 10^{-1}$.	.40

7.2	Surface plots of the spin-weighted invariant $J\bar{J}$ for time $u=1, 2, 3, 4$. The parameters of the initial data are $r_a = 3, r_b = 5, \lambda = 10^{-1}$40
7.3	Global radial angular view of $r\phi$ for time $u=0, 2, 4, 6, 8, 10$. We set $p=0, -1.2 < q < 1.2$. The parameters of the initial data are $r_a = 3, r_b = 5, \lambda = 10^{-1}$41

Abstract

In this work, we present some applications of the theory of General Relativity. First, we show a numerical scheme to account for relativistic effects in the Global Positioning System. Then, a couple of applications of astrophysical interest are worked out. These are the study of the gravitational collapse of stars and the dynamical evolution of a three-dimensional Einstein-Klein-Gordon field.

Chapter 1

Introduction

In this work, we will explore some of the applications of General Relativity. The first one is a very earthly application. It is the Global Positioning System (GPS), which has a strong presence in everyday life. Its enormous range of applications includes synchronization of power-line nodes, mapping, navigation, search and rescue, Very Long Baseline Interferometry, etc. The other two are the general relativistic description of the gravitational collapse of stars and the dynamics of a scalar field. In the case of the stars, after the nuclear fuel that powers those astronomical objects is exhausted, the stars begin a process of collapse. In general, the matter density in the late stages of such processes is so high that the Newtonian approximation is no longer valid. And for such reason, it is necessary to consider the Einstein equations to describe the evolution. In relation to the scalar field, it allows us to study situations where there is not symmetries. Thus, the study of the evolution of the scalar field gives us some insight about more complex situations.

Let talk about the GPS in first place. The technological core of GPS is formed by highly accurate, stable atomic clocks. In the GPS, the satellites send their position and exact time of transmission to the receivers on the ground. With this information, the receiver can solve a system of four simultaneous one-way signal propagation equations to determine its position. It is clear that any small error in the travel time will produce a huge error in the position because of the large value of the speed of propagation for the radio signals.

The errors in the measurement of the travel time come from different sources. For example, the electromagnetic signal sent by the satellites to the ground travels through the atmosphere. And, in the atmosphere, the speed of light is different from the speed of light on the vacuum. Additional errors come from the concept of time itself. In Newtonian Mechanics time is an absolute quantity, but that is not the case in Special Relativity. Instead, the time depends on the motion of the frames of reference. Two events or situations that

are simultaneous in a frame of reference could not be simultaneous in another. In particular, time intervals would be different. Even, the spatial separation between the events could depend on the frame of reference. Moreover, the one way signal propagation equations used in GPS are only valid in a flat space-time. They do not take in account the curvature of space-time predicted by general relativity.

Basically, the determination of the position by exchanging electromagnetic signals will be influenced by any phenomenon that affects the propagation time of electromagnetic waves or the clocks' rates. We are interested in the effects predicted by the theories of Special Relativity and General Relativity. Let us mention some of these phenomena. First, due to the relative motion between observers on the ground and the GPS satellites, the clocks on the satellites tick more slowly as seen by a ground observer. This effect is called time dilation and it depends only on the relative velocity of the satellites with respect to the ground. It makes the satellites' clocks run at a slow rate of by 7.1 ms per day. Another clock effect is the Gravitational Red Shift. General Relativity predicts that clocks closer to a massive object will tick more slowly than those located far away. Then, the clocks on the satellites appear to run faster than identical clocks on the ground. This effect causes the clocks on the satellites to run faster by 45.7 ms per day. Another effect which has a maximum value of 133ms per day for a stationary observer on the ground is the Sagnac effect. This effect is caused by the Earth rotation during the time of transit of the satellite signal from the satellite to the ground. There is also a signal propagation delay. Sometimes, this is called the Shapiro signal propagation delay. Also, the presence of spatial curvature causes a geodetic distance effect. It is related to the difference between proper distance and coordinate distance. Additional to the effects of the gravitational field of the Earth, there is a tidal potential from other bodies in the solar system that causes a gravitational frequency shift of satellite clocks of a few parts in 10^{-16} .

With the launching of the first satellite of the GPS constellation, the relevance of the predictions of the theories of Special and General Relativity became very clear. At the

level of accuracy used today in the position determination, we normally have to deal with relativistic effects such as the Doppler shift and the gravitational shift. As we mentioned before, the motion of the clocks and the gravitational field affect the clocks' rate. If we need to improve the accuracy in the position determination, then we have to include a better description of the gravitational fields and relativistic effects of higher order. To some extent, it can be a tricky task. Basically, in the GPS, the description of the orbit of the satellites and the path of the electromagnetic signals are described using Newtonian mechanics. And, all the corrections needed to account for the relativistic effects are added at the top of this Newtonian framework. We will present a different approach which may simplify that framework. We begin with an intrinsically relativistic description of the GPS. The orbits of the satellites and the path of the electromagnetic signals are calculated using the theory of General Relativity. For the relativistic description, we do not have to look on a one-by-one basis in the corrections. For example, suppose that we make an upgrade on the atomic clocks inside the GPS satellites. Then, we replace the old version of the atomic clock by a new one with an improved precision. And, If we have the right information about the gravitational field, the only thing we need to do is to increase the precision in the calculations. The calculations themselves remain the same. Even in the case that we improve the information about the gravitational field, the calculations will not change. The general idea for the scheme is that it will have only two inputs: the information about the gravitational field and the precision required for the calculations.

After our walk through the GPS, let focus our attention in the astrophysical application of general relativity. Here, we are mostly interested in the study of a spherical bulk of fluid. We will assume that the fluid is anisotropic; i.e., we allow for the radial and tangential pressures to be different. And, we will try to answer the question, Does the anisotropy have any effect in the gravitational collapse? In general, the Einstein equations are very difficult to solve. We will introduce some simplifications that make it a treatable problem without blurring the essential aspects of the problem. Basically, the method to be implemented

reduces the Einstein equations to a set of ordinary differential equations at the surface of the star. This set of equations govern the evolution of the star and the equations can be solved using standard numerical methods. The second astrophysical application is the study of the Klein-Gordon field. Here we will give the basics for evolution of a three-dimensional massless Einstein-Klein-Gordon Field.

Chapter 2

The Atmospheric Corrections in GPS

It is not our intention in this work to cover the vast and difficult task of simulating and studying the corrections that arise from the presence of the atmosphere. Here, we only give a brief description of how that problem can be solved [1].

2.1 Two Colours Laser Ranging

The main problem with electromagnetic signals propagating in the atmosphere is the uncertainty in the optical path of the signal when it moves through such dispersive medium.

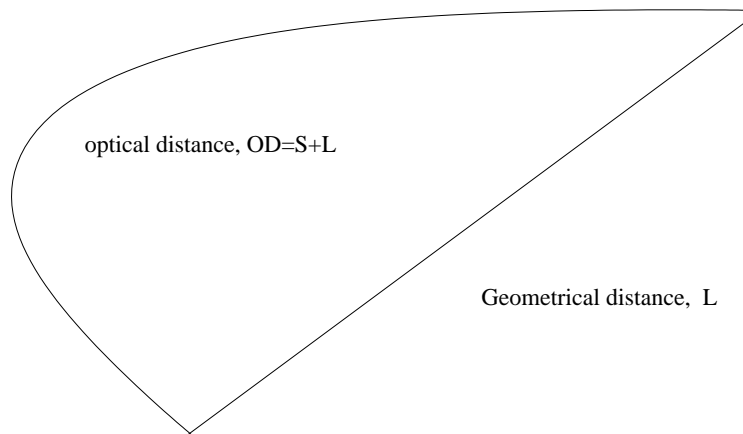


Figure 2.1: The optical and geometrical distances

As shown in the figure 2.1, The light from a laser will travel a distance OD that is larger than the true distance L. The distance S is the additional contribution due to the dispersive medium. There are two ways to estimate the value of the correction S: The first way consists in the use of accurate models of the atmosphere that allow a calculation of the path OD. The second one is the use of the “two- colours” laser.

If we denote the group velocity by V then the group index of refraction is defined by $n = \frac{c}{V}$, where c is the speed of light in the vacuum. And, the corrections for the green and

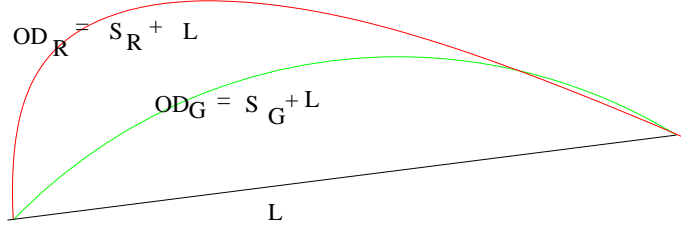


Figure 2.2: The optical paths for the two-colors laser

red laser can be written as $S_{G,R} = \int_0^L (n_{G,R} - 1) dx$. Making the difference between the two corrections, we arrive to the expression

$$\Delta S = S_G - S_R = \bar{A} \times S_R \quad (2.1)$$

where $\bar{A} = \frac{(n_G - n_R)}{(n_R - 1)}$.¹

It follows from equation (2.1) that the correction for the red laser is $S_R = \Delta S / \bar{A}$. At this point, the problem reduces to measure the difference between the red and green laser paths, ΔS . And, this difference will provide a good estimation for the corrections.

¹The indexes of refraction mentioned are actually the average indexes of refraction for the red and green laser.

Chapter 3

The Global Positioning System

In this chapter we give a general description of the Global Positioning System. We omit most of the technological details and concentrate in the relativistic part of the inner workings.

3.1 Description of the System

The Global Positioning System contains three segments [2]: a user segment, a ground segment, and a space segment. The user segment consists of all the receivers that determine the position using the GPS signals. The control segment consist of ground based tracking stations, these stations gather information about the satellites. And the space segment of the Global positioning system consists of 24 satellites distributed in six different orbital planes. Each plane forms an angle of 60 degrees with the adjacent planes and contains 4 satellites. For any of the satellites, the orbit is nearly circular with a mean altitude of 20,000 km. The speed for the satellites is approximately 4 km/s.

3.2 The Propagation Delay Equations

The positioning in the GPS is done in the following way. Satellites in orbit around the earth send their positions and time of transmission to receivers on the ground. With this information, the receiver can determine its position by solving a system of four, simultaneous, one-way signal propagation-delay equations:

$$|\vec{x}_o - \vec{x}_s|^2 - c^2(t_o - t_s)^2 = 0, \quad s = 1, 2, 3, 4. \quad (3.1)$$

Where, t_s is the time of transmission of the s -satellite's signal from the position x_s . The time and place of the reception of the signal are t_0 and x_0 , respectively. And, c is the speed of light. These equations alone will provide the position of the receiver in the case of a flat space-time. In a more general case, as in the presence of a gravitational field, we need to include the corrections for the time of flight of the satellite's signals and the corrections for the clocks' frequency offset respect to a stationary clock at rest on the ground. Here, we will deal only with corrections arising from the curvature of space-time or special relativity. And in a later chapter, we intend to replace the use of equation (3.1) by a more suitable method to find the position of GPS receivers.

3.3 Relativistic Effects on Clocks

Table 3.1: Relativistic Effects in GPS

Effect	Size of the effect, ns	Description
Gravitational Red Shift	46	orbital radius 26,650km
Time Dilation	7	Average orbital speed
Sagnag Effect	133	maximum value for a stationary receiver on the geoid
Intersatellite links	10	difference in orbital eccentricity
Earth Oblateness	0.024	additional contribution to gravitational red shift
Curvature Delay	0.002	difference between coordinate distance and proper distance
Shapiro Delay	0.003	effect on time of signal propagation
Tidal Potential	0.001	moon+sun
Lense-Thirring	0.00000003	relativistic frame dragging.

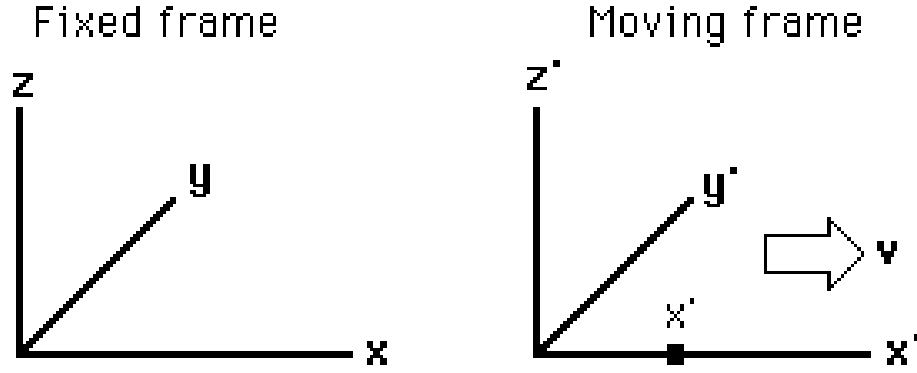


Figure 3.1: Moving reference frames

In the previous page, Table 3.1 gives a brief description of the relativistic effects that are present in GPS. The motion of the satellites and the gravitational potential affect the rate of the clocks inside the satellites. The relative motion of the satellites respect to ground stations give origin to the relativistic Doppler shift. Differences in the gravitational potential along the satellites orbit produce the so called gravitational red shift. Also, the earth rotation produces the Sagnac Effect. All these effects must be taken in account in the corrections to the timing errors. Just an error of $1ns$ gives origin to a positioning error of $30cm$.

3.3.1 Special Relativistic Effects

The main point of the special relativistic effects is that the time is not a universal quantity. Time intervals depend on the reference frame that is being used. The Lorentz transformations for the reference frames showed in figure 3.1 have the form

$$\begin{aligned}
 x' &= \gamma(x - vt), \\
 y' &= y, \\
 z' &= z, \\
 t' &= \gamma\left(t - \frac{vx}{c^2}\right).
 \end{aligned}
 \tag{3.2}$$

Where $\gamma = \frac{1}{\sqrt{1 - \frac{v^2}{c^2}}}$.

Those transformations show that a time interval $\Delta t'$ in a moving reference frame is related to the time interval Δt in a fixed frame by

$$\Delta t = \frac{\Delta t'}{\gamma}. \quad (3.3)$$

Thus, a clock onboard a satellite (moving frame) will experience a time dilation factor of γ^{-1} respect to a clock at rest on the ground (fixed frame.)

3.3.2 Gravitational Effects

3.3.2.1 The Redshift

The difference in gravitational potential between the satellite orbits and the ground level causes the satellite clocks to run faster [3],

$$\Delta t' = \frac{2(\Phi - \Phi_0)}{c^2} \Delta t. \quad (3.4)$$

Where, Φ_0 is the gravitational potential at the ground. This effect is called gravitational red shift.

3.3.2.2 The Curvature Delay

We can find the origin of this effect in the difference between the coordinate distance and the proper distance; i.e., the spatial curvature. For the GPS satellites the difference is approximately 6.3 mm.

3.3.2.3 Shapiro Delay

The effect comes from the difference between the speed of light in a flat space-time and the coordinate speed of light [4].

3.3.2.4 The Eccentricity Effect

This effect actually is a combination of the redshift and doppler effects. It originates in the fact that the orbits for the GPS satellites are not completely circular. That produces a change in velocity and altitude for the satellites along their orbits.

3.3.2.5 The Crosslink Ranging

The transfer of time information from one satellite to another by exchange of signals gives rise to this effect. The rate of the clock at the sender must be adjusted before it sends a signal to the second satellite. This signal requires a time of propagation calculation that includes relativistic time delay corrections. Then, there is another correction in the satellite that receives the signal.

Chapter 4

Fully Relativistic Description of the GPS

In this chapter, we present the basic elements needed for a relativistic description of the GPS.

4.1 The Line Element

The distance between two space-time events (x^0, x^1, x^2, x^3) and $(x^1 + dx^1, x^2 + dx^2, x^3 + dx^3, x^4 + dx^4)$ is given by

$$ds^2 = g_{\alpha\beta} dx^\alpha dx^\beta \quad (4.1)$$

The parameter s is related to the time τ measured by ideal clocks. τ is called the proper time and it is defined by

$$ds^2 = c^2 d\tau^2. \quad (4.2)$$

The line element contains all the information about the space-time. It is an invariant quantity that is related to the time measured by local observers by the relationship (4.2). Also, it gives the connection between the clocks' rates for clocks attached to different observers. Suppose that observers (a) and (b) are moving along two different paths, as show in figure 4.1. Then, for each observer

$$\left(\frac{cd\tau}{dx^0}\right)_{(a),(b)}^2 = (g_{00})_{(a),(b)} + \left(2g_{0i}\frac{dx^i}{dx^0}\right)_{(a),(b)} + \left(g_{ij}\frac{dx^i}{dx^0}\frac{dx^j}{dx^0}\right)_{(a),(b)}. \quad (4.3)$$

Looking at ratio of those two quantities , we found that the proper times for the two observer are connected by

$$\left(\frac{d\tau_{(a)}}{d\tau_{(b)}}\right)^2 = \frac{(g_{00})_{(a)} + \left(2g_{0i}\frac{dx^i}{dx^0}\right)_{(a)} + \left(g_{ij}\frac{dx^i}{dx^0}\frac{dx^j}{dx^0}\right)_{(a)}}{(g_{00})_{(b)} + \left(2g_{0i}\frac{dx^i}{dx^0}\right)_{(b)} + \left(g_{ij}\frac{dx^i}{dx^0}\frac{dx^j}{dx^0}\right)_{(b)}}. \quad (4.4)$$

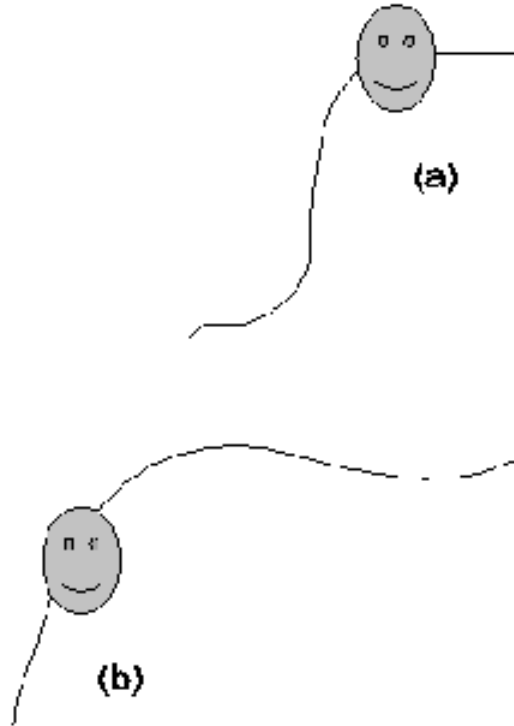


Figure 4.1: Two observer moving along different paths

4.2 Examples of the Line Element

In this section, we present some examples of the line element for different sources of the gravitational field. Each example could be considered an approximation to the true line element of the earth under the right circumstances.

4.2.1 The Schwarzschild Line Element

The line element for the space-time generated by a spherical body of mass M is given by [5]

$$ds^2 = \left(1 - \frac{R_s}{R}\right) c^2 dt^2 - \frac{dR^2}{1 - \frac{R_s}{R}} - R^2 d\theta^2 - R^2 \sin^2(\theta) d\phi^2. \quad (4.5)$$

Where, the quantity $R_s = \frac{2GM}{c^2}$ is the Schwarzschild radius.

4.2.2 The Kerr Line Element

For a rotating spherical body [6],

$$ds^2 = \left(1 - \frac{2GM}{\rho}\right) c^2 dt^2 - \frac{4GMa \sin^2(\theta)}{\rho^2} dt d\phi + \frac{\rho^2}{\Delta} dr^2 + \rho^2 d\theta^2 + \frac{\sin^2(\theta)}{\rho^2} [(r^2 + a^2)^2 - a^2 \Delta \sin^2(\theta)] d\phi^2, \quad (4.6)$$

where

$$\Delta(r) = r^2 - 2GM r + a^2 \quad (4.7)$$

and

$$\rho(r, \theta) = r^2 + a \cos^2(\theta). \quad (4.8)$$

The parameters M and a are the Komar energy and the Komar angular momentum per unit mass, respectively.

4.2.3 Line Element for an Oblate Earth

The line element for an oblate Earth [7] is obtained by a perturbation of the Schwarzschild space-time is

$$ds^2 = e^{2\lambda} dt^2 - \frac{1}{c^2} (e^{2\sigma-2\lambda} dr^2 + e^{2\sigma-2\lambda} r^2 d\theta^2 + e^{-2\lambda} r^2 \sin^2 \theta d\phi^2), \quad (4.9)$$

where σ and λ are functions of the coordinates. This line element can be considered a better approximation for the line element of the earth than the Schwarzschild line element.

4.3 Coordinates in Curved Space-Time

In the previous section, we presented several line elements that correspond to different solutions of the Einstein equations. Each solution represents a space-time for a particular matter source. These line elements are written in some particular coordinates. It is possible to write the same line element using different coordinates. In different coordinates, the line element will look different but it represents the same physical space-time as in the original coordinates.

4.3.1 Examples of Coordinates in Curved Space-Time

Let explore the coordinates in (4.5). For $R \rightarrow \infty$ the line element (4.5) reduces to $ds^2 = c^2 dt^2 - dR^2 - R^2 d\theta^2 - R^2 \sin^2(\theta) d\phi^2$. Thus, the Schwarzschild coordinates correspond to the standard spherical coordinates for large values of R . Moreover, for a static observer at large R ($dR = d\phi = d\theta = 0$) $d\tau = dt$; i.e., the Schwarzschild time coordinate t is that of a static observer in a flat space-time. Figure 4.2 and Figure 4.3 illustrate the differences between the Schwarzschild coordinates and the spherical coordinates for $R < \infty$.

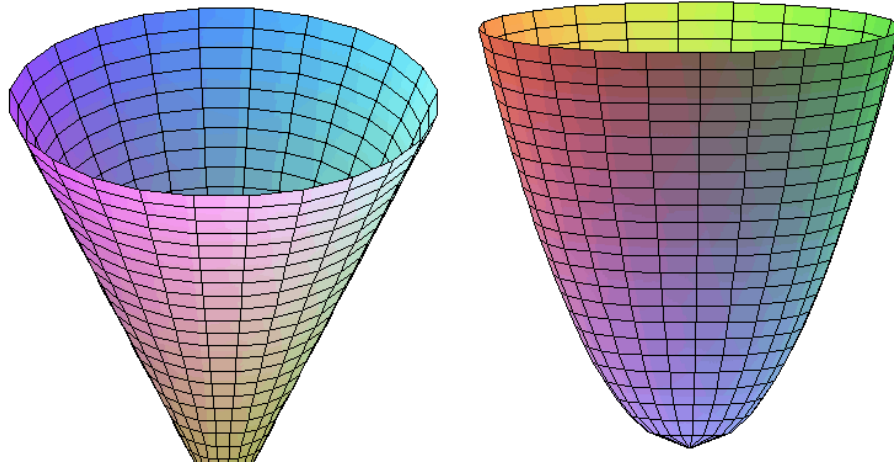


Figure 4.2: Surfaces $\theta = \text{constant}$ for a flat geometry (left) and for the Schwarzschild geometry (right)

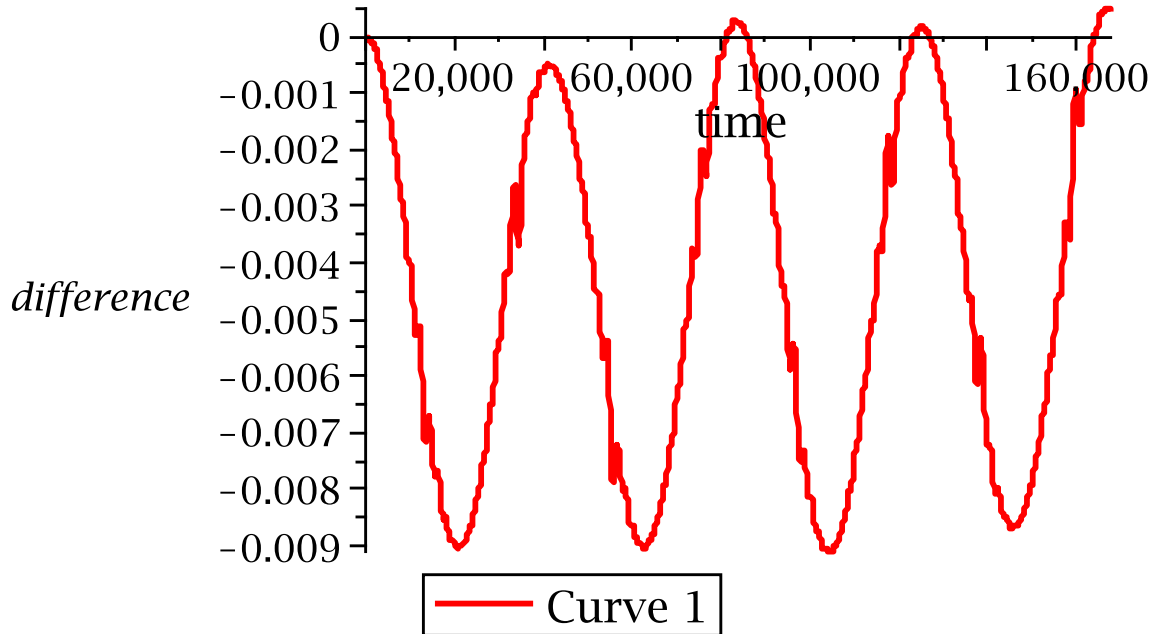


Figure 4.3: Difference, in meters, between the radial spherical coordinate and the radial Schwarzschild coordinate for a typical GPS satellite

4.4 The Proper Time and the Coordinate Time

We can use (4.4) to relate the Schwarzschild coordinate time to the proper time of any observer,

$$\left(\frac{d\tau_{\text{observer}}}{dt}\right)^2 = (g_{00})_{\text{observer}} + \left(2g_{0i}\frac{dx^i}{dx^0}\right)_{\text{observer}} + \left(g_{ij}\frac{dx^i}{dx^0}\frac{dx^j}{dx^0}\right)_{\text{observer}}. \quad (4.10)$$

4.5 The Equation of the Geodesics

In a given space-time the trajectory for a particle is described by the equation of the geodesics,

$$\frac{d^2x^\alpha}{d\tau^2} + \Gamma_{\beta\gamma}^\alpha \frac{dx^\beta}{d\tau} \frac{dx^\gamma}{d\tau} = 0. \quad (4.11)$$

In the case of photons, we need to exert some precaution because for photons $d\tau = 0$.

And, we need to replace the proper time that appears in equation (4.11) by a more convenient affine parameter λ ,

$$\frac{d^2 x^\alpha}{d\lambda^2} + \Gamma_{\sigma\rho}^\alpha \frac{dx^\sigma}{d\lambda} \frac{dx^\rho}{d\lambda} = 0. \quad (4.12)$$

4.6 The Satellite Orbits

The satellites travels along timelike geodesics. The explicit equations for the geodesics in a Schwarzschild geometry are:

$$\frac{d^2 t}{d\tau^2} + \frac{R_s}{R(R - R_s)} \frac{dt}{d\tau} \frac{dR}{d\tau} = 0 \quad (4.13)$$

$$\begin{aligned} \frac{d^2 R}{d\tau^2} + \frac{c^2 R_s (R - R_s)}{2R} \left(\frac{dt}{d\tau} \right)^2 - \frac{R_s}{2R(R - R_s)} \left(\frac{dR}{d\tau} \right)^2 \\ - (R - R_s) \left(\frac{d\theta}{d\tau} \right)^2 - \sin^2(\theta) (R - R_s) \left(\frac{d\phi}{d\tau} \right)^2 = 0 \end{aligned} \quad (4.14)$$

$$\frac{d^2 \theta}{d\tau^2} + \frac{2}{R} \frac{dR}{d\tau} \frac{d\theta}{d\tau} - \sin(\theta) \cos(\theta) \left(\frac{d\phi}{d\tau} \right)^2 = 0 \quad (4.15)$$

$$\frac{d^2 \phi}{d\tau^2} + \frac{2}{R} \frac{dR}{d\tau} \frac{d\phi}{d\tau} + 2 \frac{\cos(\theta)}{\sin(\theta)} \frac{d\theta}{d\tau} \frac{d\phi}{d\tau} = 0 \quad (4.16)$$

4.7 The Photons' Trajectory

Due to the fact that the photons travel along null geodesics. Then, we have the additional condition for null geodesics

$$ds^2 = 0. \quad (4.17)$$

Chapter 5

A Numerical Way Around the Flat Space-Time Delay Equations in GPS

We present a numerical self-consistent way to account for relativistic effects in GPS. Our approach has two main advantages with respect to the use of the traditional method of flat space-time propagation-delay equations plus relativistic corrections. At first, any improvement of our knowledge about the space-time geometry will not produce further changes in the algorithm. And second, all the relativistic effects are fully and clearly accounted for. To illustrate the ideas behind our method, we use the Schwarzschild geometry as a testbed.

5.1 The Motivation

The corrections in the time of flight of the signal come from the fact that the signals are moving on geodesics that are not longer straight lines. On the other hand, the satellite clocks' rates depend on the state of motion of the satellite plus the gravitational field.

Each of the corrections for the effects mentioned in chapter 3 are calculated one by one and taken together with equation (3.1) to find the position of the receivers. The corrections come from a series expansion of the line element written in some particular coordinates. And, each effect corresponds to some order in this series expansion. It is worth noting that the line element, that contains all the information about the geometry of space-time, is an invariant. Unfortunately, the terms in the series may not be invariants themselves. That means that if for some circumstance we switch coordinates then we need to be careful enough to write the corrections in the new coordinates. In this work, we will show how we can replace equation (3.1) plus corrections by an iterative numerical method that contains no explicit corrections. The idea is to use the equation of the geodesics to describe the motion of the satellites and the propagation of the signals. Here, we are going to replace the use of the proper time for

each satellite by the coordinate time. Everything will be described by this special observer at infinity. That means we go from synchronizing clocks to providing the initial conditions for the coordinates. This way, we don't need to keep track of the different time rates for different clocks.

5.2 Sending the Initial Conditions

The observer at infinity can send a signal to some specific point in the trajectory of the satellites. If we use the condition (4.17) and equation (4.1), we obtain

$$\int c dt = \int dt \sqrt{(2g_{0i} \frac{dx^i}{dt}) + (g_{ij} \frac{dx^i}{dt} \frac{dx^j}{dt})}, \quad (5.1)$$

$$dx^0 = dt.$$

These equations give the (coordinate) time it takes to the signal to travel from the observer at infinity to the satellite. This way the satellite knows the initial conditions for its four coordinates. And, the equations of the geodesic can be integrated.

5.3 Positioning in Curved Space-time

As we mentioned before, each GPS satellite broadcasts its position and time of transmission of the signal. We will assume that the satellites send their time-like coordinate x^0 instead of their proper time. Then, using the four space-time coordinates of the satellite as initial conditions, it is possible to integrate equation (4.12) to find points that lie on the wavefront (see Figure 5.1) at the time given by the coordinate time x^0 . And, we can use some interpolation scheme to reconstruct the rest of the wavefront. After we have reconstructed the four wavefronts corresponding to the four satellites, we proceed to find the point where they intersect.

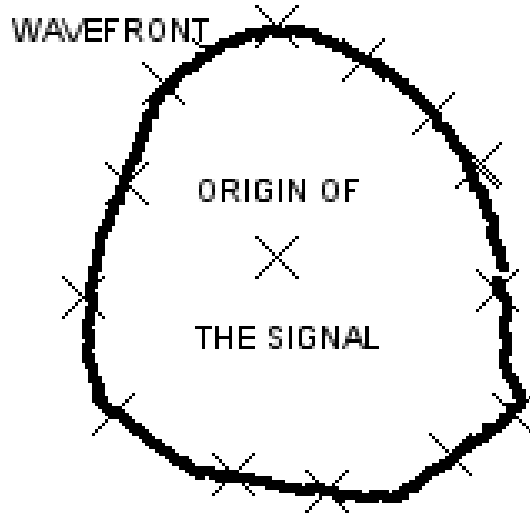


Figure 5.1: The wavefront for the signals

We used a Runge-Kutta integrator to solve the equations of the geodesics and Chebychev interpolating polynomials to reconstruct the wavefronts.

We can list the step of our schema as:

- Get the initial conditions from the observer at infinity.
- Integrate the equation of the geodesics to find the orbits of the satellites. This will provide the coordinates x^α for each satellite as functions of the proper time τ .
- Using the equations of the geodesics for the photons emitted from the satellites and the coordinates of the satellites, find a set of points that lie on the wavefronts.
- Using the points that lie on the wavefronts, make a piecewise reconstruction of the wavefronts.
- After we have the reconstruction of the wavefronts, find the point that is the closest point to all four wavefronts. This point will give the position of the receiver.

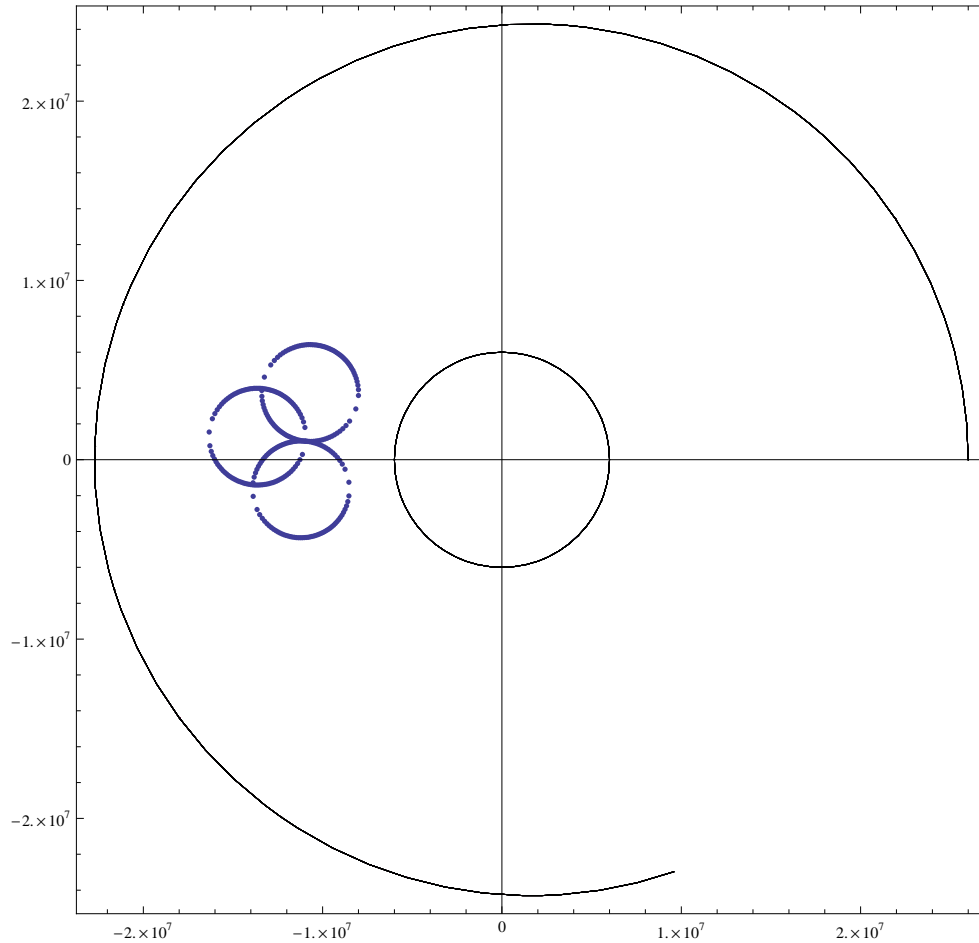


Figure 5.2: Numerical reconstruction of the wavefronts, all the distances are expressed in meters

5.4 An Example

As an example, we will consider the localization of a receiver in a Schwarzschild space-time. Figure 5.2 shows a typical orbit for a GPS satellite (large black curve), the spherical Earth (small black curve) and the reconstructed wavefronts (blue curves.)

Figure 5.3 illustrates the search for the closest points. After those points are found, it is possible to make an interpolation to increase the precision. The size of the distances between the closest points will give an indication of the error in the position.

This scheme to find the position is not the most elegant of all methods. But, it shows that is possible to go around the propagation delay equations and its relativistic corrections.

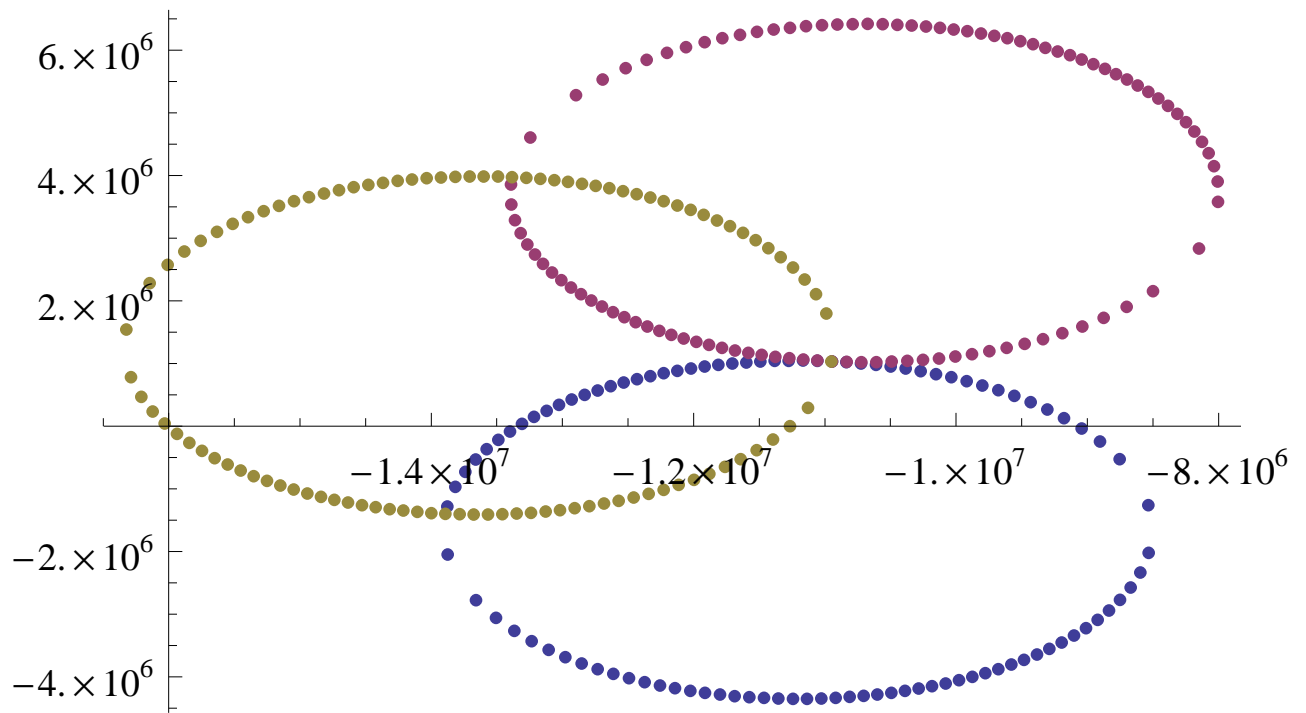


Figure 5.3: Search for the closest point to the wavefronts, all the distances are expressed in meters

Chapter 6

Evolution of Anisotropic Stars

The Einstein field equations, $G_{\mu\nu} = 8\pi T_{\mu\nu}$ (geometrized units,) relate the geometry of the space-time to its energy and matter content. This set of equations specify all the possible space-times. In this chapter, we solve the Einstein equations for an anisotropic and spherically shaped bulk of fluid.

6.1 The Energy-momentum Tensor

We describe the star using the following variables: the radial pressure P_r , the tangential pressure P_\perp , the energy density ρ , the free streaming ϵ , the heat flux q and the four velocity $U^\mu = (U^t, U^r, 0, 0)$.

$$\begin{aligned}
 T^{\mu\nu} = & \rho U^\mu U^\nu + P_\perp (U^\mu U^\nu - g^{\mu\nu} - S^\mu S^\nu) + P_r S^\mu S^\nu \\
 & + \epsilon (U^\mu U^\nu + S^\mu S^\nu + S^\mu U^\nu + U^\mu S^\nu) + q (S^\mu U^\nu + U^\mu S^\nu).
 \end{aligned}
 \tag{6.1}$$

Where the vectors S^μ and U^μ satisfy

$$\begin{aligned}
 S^\mu U_\mu &= 0, \\
 S^\mu S_\mu &= -1, \\
 U^\mu U_\mu &= +1.
 \end{aligned}
 \tag{6.2}$$

For a local observer comoving with the fluid, the energy-momentum tensor takes the form

$$\begin{pmatrix}
 \rho + \epsilon & -\epsilon - q & 0 & 0 \\
 -\epsilon - q & p_r + \epsilon & 0 & 0 \\
 0 & 0 & p_\perp & 0 \\
 0 & 0 & 0 & p_\perp
 \end{pmatrix}.
 \tag{6.3}$$

6.2 The Effective Variables

It is convenient to define the quantities effective density $\tilde{\rho}$ and effective pressure \tilde{P} by means of

$$\tilde{\rho} \equiv T_0^0 = \frac{\rho + \omega^2 P_r + 2\omega q + (1 + \omega)^2 \epsilon}{1 - \omega^2}, \quad (6.4)$$

$$\tilde{P} \equiv T_1^1 = \frac{\omega^2 \rho + P_r + 2\omega q + (1 + \omega)^2 \epsilon}{1 - \omega^2}. \quad (6.5)$$

These quantities satisfy the conditions

$$\tilde{\rho} - \tilde{P} = \rho - P_r \quad (6.6)$$

and

$$\tilde{\rho}_{static} = \rho \quad \tilde{P}_{static} = P_r. \quad (6.7)$$

6.3 The Interior Line Element in Schwarzschild Coordinates

In Schwarzschild coordinates, the line element inside the fluid takes the form [8],

$$ds_-^2 = e^\nu dt^2 - e^\lambda dr^2 - r^2 (d\theta^2 + \sin^2 \theta d\phi^2). \quad (6.8)$$

For a spherically symmetric space-time, the variables ν and λ are functions of the coordinates r and t .

6.4 The Exterior Line Element

For the exterior of the fluid, due to the presence of radiation, the spacetime is that of Vaidya [9]

$$ds_+^2 = \left(1 - \frac{2M(t)}{r}\right) dt^2 - \left(1 - \frac{2M(t)}{r}\right)^{-1} dr^2 - r^2 (d\theta^2 + \sin^2 \theta d\phi^2). \quad (6.9)$$

6.5 The Explicit Form for U^μ and S^μ

In order to find the explicit form for U^μ and S^μ , it is necessary to introduce the local Minkowski coordinates (T, x, θ, ϕ) ,

$$\begin{aligned} dT &= e^{\nu/2} dt, \\ dx &= e^{\lambda/2} dr, \\ dy &= r d\theta, \\ dz &= r \sin \theta d\phi. \end{aligned} \quad (6.10)$$

And, the Lorentz transformations to a reference frame moving with velocity ω respect to (6.10)

$$\begin{aligned} dT' &= \gamma(dT - \omega dx), \\ dx' &= \gamma(dx - \omega dT), \\ dy' &= dy, \\ dz' &= dz. \end{aligned} \quad (6.11)$$

Where, $\gamma = \frac{1}{\sqrt{1 - \omega^2}}$.

In the comoving frame, the velocity of the fluid is zero and the four-velocity is defined as

$$U^\mu = (1, 0, 0, 0) = U_\mu \quad (6.12)$$

and the vector

$$S^\mu = (S^t, S^r, 0, 0). \quad (6.13)$$

Taking in account the conditions (6.2), we find that

$$S^\mu = (0, 1, 0, 0). \quad (6.14)$$

Now, the transformations (6.11) and (6.10) imply

$$U^\mu = \left(\frac{e^{-\nu/2}}{\sqrt{1-\omega^2}}, \frac{\omega e^{-\lambda/2}}{\sqrt{1-\omega^2}}, 0, 0 \right) \quad (6.15)$$

and

$$S^\mu = \left(\frac{\omega e^{-\nu/2}}{\sqrt{1-\omega^2}}, \frac{e^{-\lambda/2}}{\sqrt{1-\omega^2}}, 0, 0 \right). \quad (6.16)$$

We also get an equation for the coordinate velocity

$$\frac{dr}{dt} = e^{(\nu-\lambda)/2} \omega \quad (6.17)$$

6.6 The Einstein Field Equations

Using the interior line element ds_-^2 and the explicit form for the vectors U^μ and S^μ , we can write the Einstein equations as,

$$-\frac{e^\lambda - 1 + \lambda_{,r}r}{r^2 e^\lambda} = 8\pi \frac{1}{1-\omega^2} (\rho + \omega^2 P_r + 2\omega q + (1+\omega)^2 \epsilon), \quad (6.18)$$

$$-\frac{\lambda_{,t}}{e^\nu r} = -8\pi \frac{e^{(\lambda-\nu)/2}}{1-\omega^2} (\omega \rho + \omega P_r + (1+\omega^2)q + (1+\omega)^2 \epsilon), \quad (6.19)$$

$$-\frac{e^\lambda - 1 - \nu_{,r}r}{e^{\lambda}r^2} = -8\pi \frac{1}{1 - \omega^2} (\omega^2 \rho + P_r + 2\omega q + (1 + \omega)^2 \epsilon), \quad (6.20)$$

$$\begin{aligned} -8\pi P_\perp = & -\frac{1}{4re^\nu e^\lambda} (2\lambda_r e^\nu - 2\nu_r e^\nu + 2r\lambda_{,tt}e^\lambda + r\lambda_{,t}^2 e^\lambda \\ & - r\nu_{,r}^2 e^\nu - 2r\nu_{,rr}e^\nu + r\nu_{,r}e^\nu \lambda_{,r} - r\nu_{,t}\lambda_{,t}e^\lambda). \end{aligned} \quad (6.21)$$

6.7 The Junction Conditions

Given two regions, R and \bar{R} , of the space-time with a common boundary S . Assume that each region has its own line element, g , and coordinates, x , and that the boundary is described by

$$f(x^\mu) = 0 \quad \text{in } R \quad (6.22)$$

and

$$\bar{f}(\bar{x}^\mu) = 0 \quad \text{in } \bar{R}. \quad (6.23)$$

Then, the normal vectors to the boundary are defined by

$$n_\mu = \frac{f_{,\mu}}{\sqrt{g^{\mu\nu} f_{,\mu} f_{,\nu}}} \quad \text{in } R \quad (6.24)$$

and

$$\bar{n}_\mu = \frac{\bar{f}_{,\mu}}{\sqrt{\bar{g}^{\mu\nu} \bar{f}_{,\mu} \bar{f}_{,\nu}}} \quad \text{in } \bar{R}. \quad (6.25)$$

We can get a smooth coupling of the regions across the boundary S if [10]

1. The first fundamental form is continuous across S : $[g_{\mu\nu}]_- = [g_{\mu\nu}]_+$.
2. The second fundamental form is continuous across S : $[\hat{n}_{\mu;\nu}]_- = [\hat{n}_{\mu;\nu}]_+$.

Using the line elements (6.8) and (6.9), those conditions (at the surface of the star) translate into

1. $e^{\nu_a} = 1 - 2\frac{M(t)}{a(t)} = e^{-\lambda_a}$ (first fundamental form at $r = a$.)
2. $\tilde{P}_a = -\omega_a\tilde{\rho}_a$ (second fundamental form at $r = a$.)

6.8 The Method of the Effective Variables

We can introduce the new variable m through

$$e^{-\lambda} = 1 - 2\frac{m}{r}. \quad (6.26)$$

Then, after integrating (6.18) and (6.20), we obtain

$$m_{static} = \int 4\pi r^2 \rho dr \quad m_{dynamic} = \int 4\pi r^2 \tilde{\rho} dr, \quad (6.27)$$

and

$$\nu_{static} = \int \frac{2m_{static} + 8\pi r^3 P_{r_{static}}}{r^2 - 2m_{static}r} dr, \quad (6.28)$$

$$\nu_{dynamic} = \int \frac{2m_{dynamic} + 8\pi r^3 \tilde{P}}{r^2 - 2m_{dynamic}r} dr. \quad (6.29)$$

Where, static means $\omega = 0$ ($q = 0$, $\epsilon = 0$) and dynamic is the case $\omega \neq 0$.

It is worth to mention that m and ν have the same functional form for both the static and the dynamic case. And, by virtue of (6.7), the dynamic case reduces to the static one for $\omega = 0$, $\epsilon = 0$. This fact allow us to use the following scheme to solve the Einstein equations [11]:

1. Find a static solution to the Einstein equations.
2. Assume that the radial dependence for $\tilde{\rho}$ and \tilde{P} is the same as the radial dependence for ρ and P .
3. Take in account the junction conditions.
4. Get ν and m (or λ) from (6.29) and (6.27) , respectively.
5. Assume that the parameters that appear in the previous integration are functions of the time.
6. Solve the following set of differential equations for those functions:
 - (a) Equation (6.17) evaluated at the surface($r = a$.)
 - (b) Equation (6.19) evaluated at $r = a$.
 - (c) Equation of the energy-momentum conservation, $T_{1;\nu}^{\mu} = 0$,evaluated at $r = a$.
7. Obtain algebraically the pressure, density, velocity from the field equations.

6.9 The Equations at the Surface ($r=a(t)$)

- Equation (6.17) evaluated at the surface

$$\dot{a} = \omega_a \left(1 - \frac{2m_a}{a} \right) \quad (6.30)$$

- Equation (6.19) evaluated at the surface, gives an equation for $\dot{\omega}$.

$$\dot{m}_a = -4\pi a^2 \left(1 - \frac{2m_a}{a}\right) (1 + \omega_a)(q + \epsilon) \quad (6.31)$$

- The energy-momentum conservation equation

$$\begin{aligned} \tilde{P}_{,r} + \frac{(\tilde{\rho} + \tilde{P})(4\pi r^3 \tilde{P} + m)}{r^2 - 2mr} = \frac{e^{-\nu}}{4\pi r(r - 2m)} \left(m_{,tt} + \frac{3m_{,t}^2}{r - 2m} \right. \\ \left. - \frac{m_{,t}\nu_{,t}}{2} \right) + \frac{2}{r} (P_{\perp} - \tilde{P}) \end{aligned} \quad (6.32)$$

6.10 A Model

For the static model, we choose

$$\rho = \frac{3}{56\pi r^2}. \quad (6.33)$$

Then, using (6.27) and (6.32) for the static case, we obtain for the static pressure

$$\begin{aligned} P_r = \frac{1}{56\pi h r^2} \left(8 - 3h + 4 \tan \left(-\frac{1}{2} \ln(r) \sqrt{-4 + 3h} + \frac{1}{2} \sqrt{-4 + 3h} \ln(a) \right. \right. \\ \left. \left. + \arctan \left(\frac{1 - 8 + 3h}{4 \sqrt{-4 + 3h}} \right) \right) \sqrt{-4 + 3h} \right). \end{aligned} \quad (6.34)$$

Obtaining (6.34), we used the equation of state [12]

$$P_{\perp} - P_r = \frac{1 - h}{4} r \frac{d\nu}{dr} (\rho + P_r). \quad (6.35)$$

This equation of state allows us to write equation (6.32) for the static case in a very simple way,

$$\frac{dP_r}{dr} = -\frac{h}{2} (\rho + P_r) \frac{d\nu}{dr}, \quad (6.36)$$

where $h \geq \frac{4}{3}$.

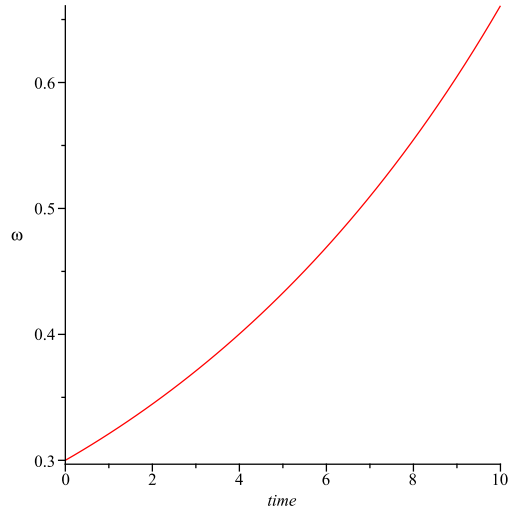


Figure 6.1: Evolution of ω for $h=1.34$

6.11 The Evolution

The following figures show the evolution of the fluid for different values of the parameter h and the same initial conditions ($a(0) = 10$, $m(0) = 2.5$, $\omega(0) = 0.3$). From the behavior of the velocity ω , we can infer that the explosion of the star is faster for increasing values of the parameter h and the increase in the initial mass favors the collapse.

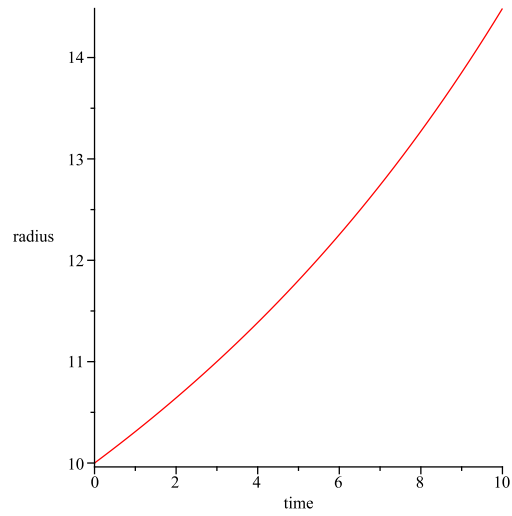


Figure 6.2: Evolution of the radius for $h=1.34$

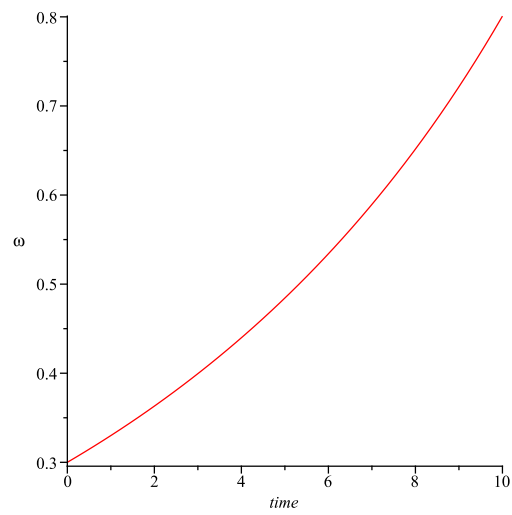


Figure 6.3: Evolution of ω for $h=1.54$

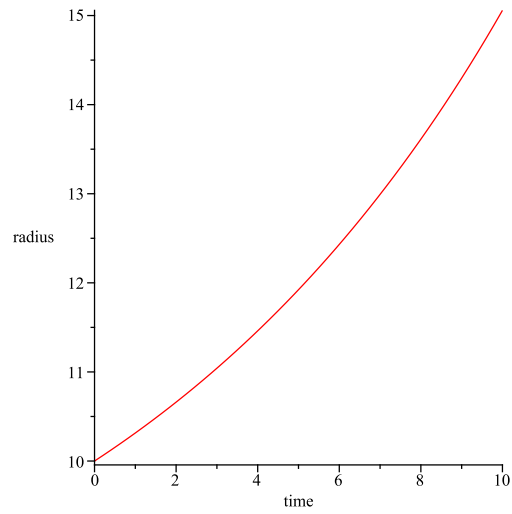


Figure 6.4: Evolution of the radius for $h=1.54$

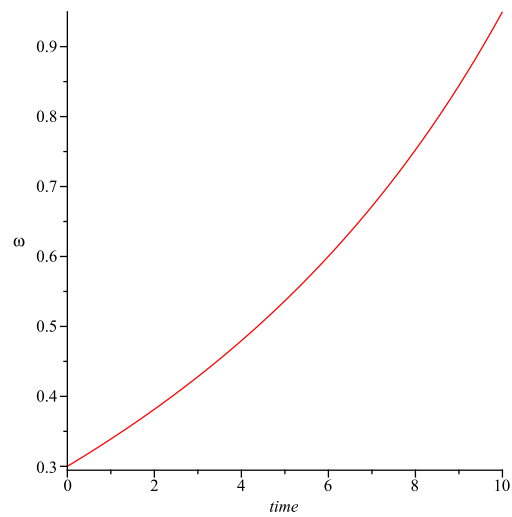


Figure 6.5: Evolution of ω for $h=1.74$

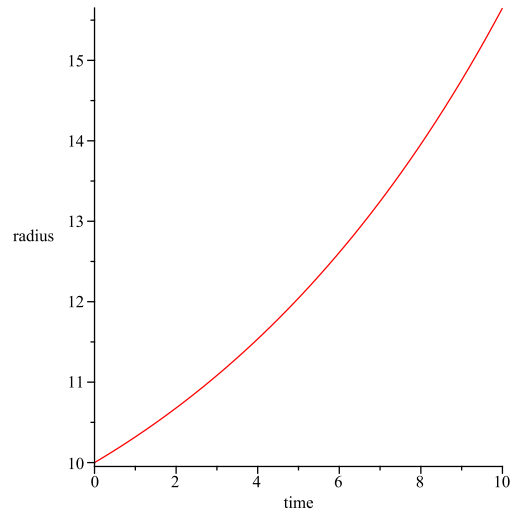


Figure 6.6: Evolution of the radius $h=1.74$

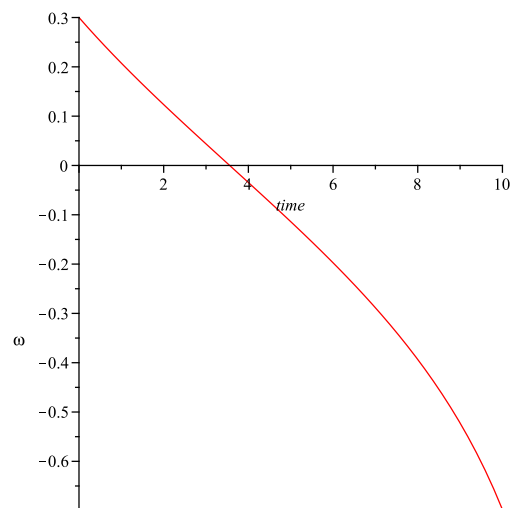


Figure 6.7: Evolution of ω for $h=1.74$, $m(0)=9.9$

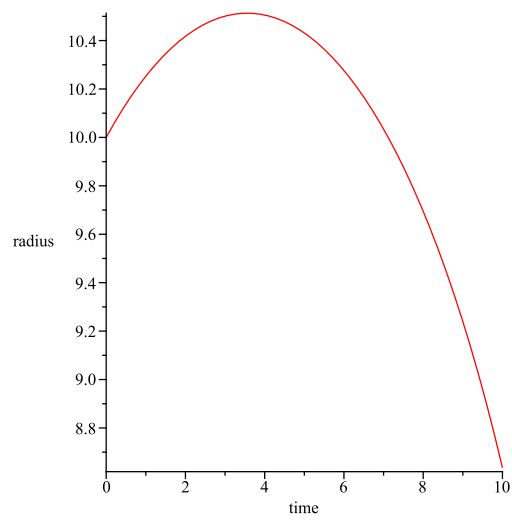


Figure 6.8: Evolution of the radius for $h=1.74$, $m(0)=9.9$

Chapter 7

The Klein-Gordon Field

In this chapter, we present the basic elements for the study of the evolution of a Klein-Gordon field. Most of the work is based in the publication [13].

7.1 The Stress Tensor for the Klein-Gordon Field

The stress tensor for the Klein-Gordon field is [14]

$$T_{ab} = \nabla_a \phi \nabla_b \phi - \frac{1}{2} g_{ab} (\nabla_c \phi \nabla^c \phi + m^2 \phi^2) \quad (7.1)$$

and it satisfies the conservation equation

$$\nabla^a T_{ab} = 0. \quad (7.2)$$

7.2 The Klein-Gordon Equation

The wave equation for the field in a flat space-time can be generalized to curved space-time using the rule [14]

$$\begin{aligned} \eta_{ab} &\rightarrow g_{ab}, \\ \partial_a &\rightarrow \nabla_a. \end{aligned} \quad (7.3)$$

Thus, we obtain

$$\nabla^a \nabla_a \phi - m^2 \phi = 0. \quad (7.4)$$

7.3 The Metric

We will use a coordinate system based on outgoing null hypersurfaces. The label for the hypersurfaces is u , x^A ($A=1,2$) will label the null rays, and r is a surface area coordinate.

Then, in the coordinates (u, r, x^A) , the metric takes the Bondi-Sachs form

$$\begin{aligned} ds^2 = & - \left(\exp(2\beta) \left(1 + \frac{W}{r} \right) - r^2 h_{AB} U^A U^B \right) du^2 \\ & - 2 \exp(2\beta) dudr - 2r^2 h_{AB} U^B dudx^A + r^2 h_{AB} dx^A dx^B. \end{aligned} \quad (7.5)$$

Where W is related to the more usual Bondi-Sach variable V by $V = r+W$, and $h^{AB} h_{BC} = \delta_C^A$ and $\det(h_{AB}) = \det(q_{AB})$, with q_{AB} a unit sphere metric. We also use the intermediate

variable $Q_A = r^2 \exp(-2\beta) h_{AB} U_r^B$. We will work in the stereographic coordinates $x^A = (p, q)$. In these coordinates the sphere metric takes the form $q_{AB} dx^A dx^B = \frac{4}{P^2} (dq^2 + dp^2)$, where $P = 1 + p^2 + q^2$. And, it is useful to introduce the complex dyad $q_A = \frac{P}{2}(1, i)$. Then, h_{AB} can be represented by its dyad component $J = \frac{1}{2} h_{AB} q^A q^B$ and $K = \frac{1}{2} h_{AB} q^A \bar{q}^B$. The two quantities J and K satisfy the relationship $1 = K^2 - J\bar{J}$. We can also introduce the spin-weighted fields $U = U^A q_A$ and $Q = Q_A q^A$.

7.4 The Field Equations

The field equations for a real, massless scalar field coupled minimally to gravity are

$$R_{ab} = 8\pi \phi_{,a} \phi_{,b}. \quad (7.6)$$

The corresponding Bondi-Sachs hypersurface equations are

$$\beta_{,r} = 2\pi r \phi_{,r}^2 + N_\beta, \quad (7.7)$$

$$(r^2 Q)_{,r} = 16\pi r^2 \phi_{,r} \bar{\partial} \phi - r^2 (\bar{\partial} J + \bar{\partial} K)_{,r} + 2r^2 \bar{\partial} \left(\frac{\beta}{r^2} \right)_{,r} + N_Q, \quad (7.8)$$

$$U_{,r} = \frac{\exp(2\beta)}{r^2} (QK - J\bar{Q}), \quad (7.9)$$

$$\begin{aligned} W_{,r} = & 2\pi \exp(2\beta) (2K \bar{\partial} \phi \bar{\partial} \phi - J (\bar{\partial} \phi)^2 - \bar{J} (\partial \phi)^2) + \frac{1}{2} \exp(2\beta) \mathcal{R} \\ & - 1 - \exp(\beta) \bar{\partial} \bar{\partial} \exp(\beta) + \frac{1}{4r^2} (r^4 (\bar{\partial} \bar{U} + \bar{\partial} U))_{,r} + N_W, \end{aligned} \quad (7.10)$$

where

$$\mathcal{R} = 2K - \bar{\partial} \bar{\partial} K + \frac{1}{2} (\bar{\partial}^2 J + \bar{\partial}^2 \bar{J}) + \frac{1}{4K} (\bar{\partial} \bar{J} \bar{\partial} J - \bar{\partial} J \bar{\partial} \bar{J}). \quad (7.11)$$

And the evolution equations for J is

$$\begin{aligned} 2(rJ)_{,ur} - \left(\frac{V}{r} (rJ)_{,r} \right)_{,r} = & \frac{8\pi}{r} \exp(2\beta) (\bar{\partial} \phi)^2 - \frac{1}{r} (r^2 \bar{\partial} U)_{,r} \\ & + \frac{2}{r} \exp(\beta) \bar{\partial}^2 \exp(\beta) - \left(\frac{W}{r} \right)_{,r} J + N_J. \end{aligned} \quad (7.12)$$

All the quantities N_β , N_Q , N_W , and N_J can be found in [15].

The wave equation for the scalar field is

$$2(r\phi)_{,ur} - \left(\frac{V}{r} (r\phi)_{,r} \right)_{,r} = - \left(\frac{W}{r} \right)_{,r} \phi + N_\phi \quad (7.13)$$

where

$$N_\phi = \frac{\exp(2\beta)}{r} (N_{\phi 1} - N_{\phi 2} + N_{\phi 3}) - \frac{r}{2} N_{\phi 4} - N_{\phi 5}, \quad (7.14)$$

$$N_{\phi 1} = K (\partial\bar{\partial}\phi + \bar{\partial}\beta\bar{\partial}\phi + \bar{\partial}\beta\bar{\partial}\phi), \quad (7.15)$$

$$N_{\phi 2} = \frac{1}{2} (\partial J\bar{\partial}\phi + \bar{\partial} J\partial\phi + 2 (J\bar{\partial}\beta\bar{\partial}\phi + \bar{J}\partial\beta\partial\phi) + J\bar{\partial}^2\phi + \bar{J}\partial^2\phi), \quad (7.16)$$

$$N_{\phi 3} = \frac{1}{4K} (\bar{J}\bar{\partial} J\bar{\partial}\phi + J\bar{\partial} \bar{J}\partial\phi + \bar{J}\partial J\bar{\partial}\phi + J\bar{\partial} \bar{J}\partial\phi), \quad (7.17)$$

$$N_{\phi 4} = \phi_{,r} (\bar{\partial}U + \partial\bar{U}) + 2 (U\bar{\partial}\phi_{,r} + \bar{U}\partial\phi_{,r}) + \bar{U}_{,r}\bar{\partial}\phi + U_{,r}\partial\phi, \quad (7.18)$$

and

$$N_{\phi 5} = U\bar{\partial}\phi + \bar{U}\partial\phi. \quad (7.19)$$

7.5 Numerical Implementation

To solve the field equations we use a method based on a second-order accurate finite difference approximation.

7.5.1 Numerical Grid

We can define a grid with coordinates $(u_n, x_i, q_j, p_k) = (n\Delta u, \frac{1}{2} + (i-1)\Delta x, -1 + (j+3)\Delta q, -1 + (k+3)\Delta p)$. Here the spatial indexes range from $i = 1, N_x, (j, k) = 1, N_\zeta, 2\Delta x = \frac{1}{N_x - 1}$, and $\Delta q = \Delta p = \frac{2}{N_\zeta - 5}$. For stability reasons, we center the derivatives at midpoint of the cell and the evolution is carried out subject to the Courant-Friedrichs-Levy condition.

7.5.2 Evolution Equations

To solve the evolution equations, we use a Crank-Nicholson scheme and the finite difference version of the equations. Also, we employ the null parallelogram marching algorithm. The wave equation can be rewritten in terms of the two dimensional wave operator

$$\square^{(2)}(r\phi) = \exp(-2\beta) \left(2(r\phi)_{,ru} - (r^{-1}V(r\phi)_{,r})_{,r} \right) \quad (7.20)$$

that correspond to the line element

$$d\sigma^2 = \exp(2\beta) (r^{-1}V du + 2dr). \quad (7.21)$$

The evolution equations then reduce to

$$\exp(2\beta)\square^{(2)}(r\phi) = \mathcal{H} \quad (7.22)$$

where

$$\mathcal{H} = - \left(\frac{W}{r} \right)_{,r} \phi + N_\phi. \quad (7.23)$$

The two-dimensional wave operator is conformally flat of weight -2. This fact allows us to use an identity relating the values of $r\phi$ at the corners P, Q, R, S of a null parallelogram

$$(r\phi)_Q = (r\phi)_P + (r\phi)_S - (r\phi)_R + \frac{1}{2} \int_{\mathcal{A}} \mathcal{H} dudr. \quad (7.24)$$

By approximating the integrand in (7.24) by its value at the center of the parallelogram, we obtain

$$(r\phi)_Q = (r\phi)_P + (r\phi)_S - (r\phi)_R + \frac{1}{2} \Delta u (r_Q - r_P - r_S - r_R) \mathcal{H}_C \quad (7.25)$$

Where \mathcal{H}_C is the value of \mathcal{H} at the center.

7.5.3 Scattering of Massless Scalar Field

We evolve the initial data

$$r\phi(u=0, r, q, p) = \begin{cases} \lambda(r-r_a)^4(r-r_b)^4 G(q, p) & \text{if } r \in [R_a, R_b], \\ 0 & \text{otherwise} \end{cases} \quad (7.26)$$

where $G(q, p) = \left[\frac{q^2 + p^2 - 0.4}{q^2 + p^2 + 1} \right]^4$. This is an axisymmetric scalar field.

Figures 7.5.3 and 7.5.3 shows the evolution of $r\phi$ and the invariant $J\bar{J}$. Figure 7.5.3 show the angular slice view for $p=0$.

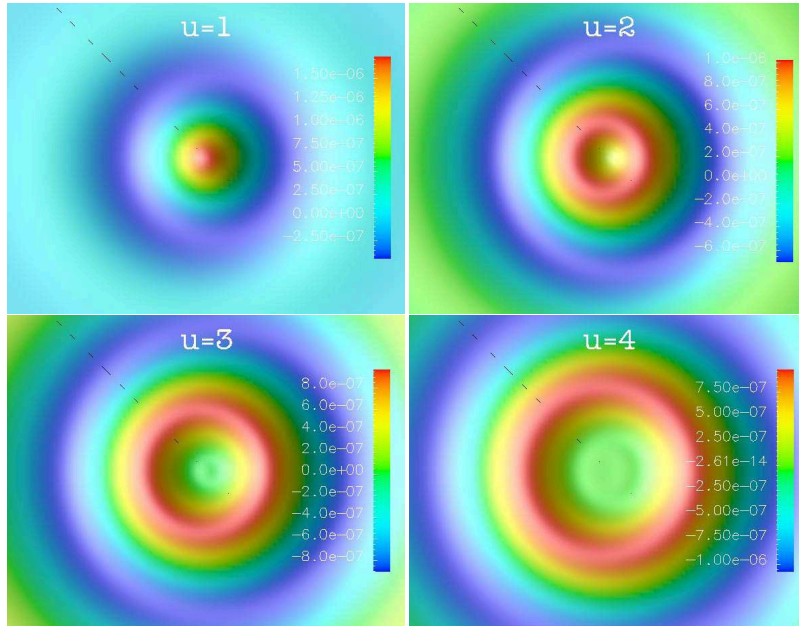


Figure 7.1: Axisymmetric surface plots of $r\phi$ for time $u=1, 2, 3, 4$. The parameters of the initial data are $r_a = 3$, $r_b = 5$, $\lambda = 10^{-1}$.

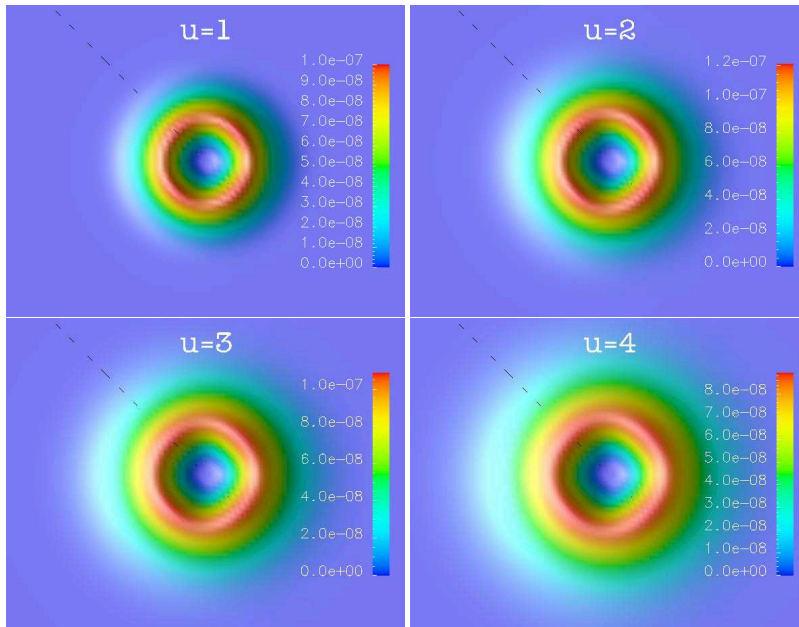


Figure 7.2: Surface plots of the spin-weighted invariant $J\bar{J}$ for time $u=1, 2, 3, 4$. The parameters of the initial data are $r_a = 3$, $r_b = 5$, $\lambda = 10^{-1}$.

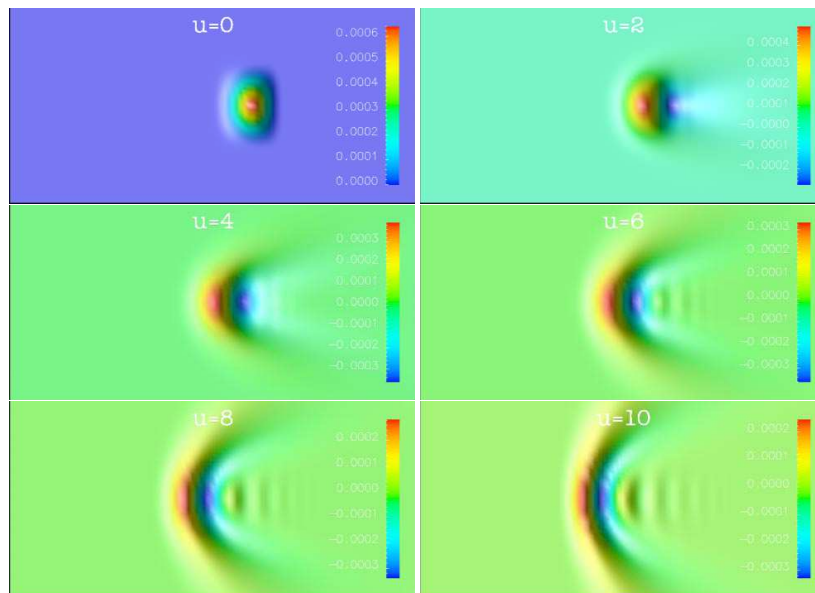


Figure 7.3: Global radial angular view of $r\phi$ for time $u=0, 2, 4, 6, 8, 10$. We set $p=0$, $-1.2 < q < 1.2$. The parameters of the initial data are $r_a = 3$, $r_b = 5$, $\lambda = 10^{-1}$.

Bibliography

- [1] Bender L and Owens J. Correction of optical distance measurements for the fluctuating atmospheric index of refraction. *Journal of Geophysical Research*, 70(10), 1965.
- [2] Ashby N. Relativity in the global positioning system. *Living Reviews in Relativity*, 6(2003-1ashby), 2003.
- [3] Einstein A. Über den einfluss der schwerkraft auf die ausbreitung des lichtetes. *Annalen der Physik*, 35, 1911.
- [4] Shapiro I, Pettengill G, Ash M, Stone M, Smith W, Ingalls R, and Brockelman R. Fourth test of general relativity: Preliminary results. *Physical Review Letters*, 20, May 1968.
- [5] Schwarzschild K. Über das gravitationsfeld eines massenpunktes nach der einstein'schen theorie. *Sitzungsberichte der Koniglich Preussischen Akademie der Wissenschaften*, 1, 1916.
- [6] Kerr RP. Gravitational field of a spinning mass as an example of algebraically special metrics. *Physical Review Letters*, 11(5), 1963.
- [7] Geisler P and McVittie G. The metric for the gravitational field of the oblate earth and the equatorial orbits of a satellite. *Montly Notices of the Royal Astronomical Society*, 131, 1966.
- [8] d'Inverno R. *Introducing Einstein's Relativity*. first edition, 1998.
- [9] Lindquist R, Schwartz R, and Misner C. Vaidya's radiating schwarzschild metric. *Physical Review*, 137(5B), March 1965.
- [10] Herrera L and Jimenez J. Junction conditions and the propagation of isometries in general relativity. *Physical Review D*, 28(12), 1983.
- [11] Herrera L, Jimenez J, and Ruggeri G. Evolution of radiating fluid spheres in general relativity. *Physical Review D*, 22(10), 1980.
- [12] Cosenza M, Herrera L, Esculpi M, and Witten L. Some models of anisotropic spheres in general relativity. *Journal of Mathematical Physics*, 22(1), 1981.
- [13] Barreto W, Da Silva A, Gomez R, Lehner L, Rosales L, and Winicour J. Three-dimensional einstein-klein-gordon system in characteistic numerical relativity. *Physical Review D*, 71, 2005.
- [14] Wald R. *General Relativity*. University of Chicago Press, first edition, 1984.
- [15] Bishop N, Gomez R, Lehner L, and Winicour W. High-powered gravitational waves. *Physical Review D*, 54(10), 1997.

Appendix: Permission to Use Copyrighted Material

From APS Copyright Policies and Frequently Asked Questions (<http://publish.aps.org/copyrightFAQ.html>)

- **As the author of an APS-published article, may I post my article or a portion of my article on my own website?** Yes, the author or the author's employer may use all or part of the APS published article, including the APS-prepared version (e.g., the PDF from the online journal) without revision or modification, on the author's or employer's website as long as a fee is not charged. If a fee is charged, then APS permission must be sought. In all cases, the appropriate bibliographic citation and notice of the APS copyright must be included.
- **As the author of an APS-published article, will I hold copyright to a "derived work", as described above, even if the original article was published prior to 1 October 2008?** Yes. The APS will extend this author right to all papers published in APS journals.
- **As the author of an APS-published article, may I use figures, tables, graphs, etc. in future publications?** Yes, as the author you have the right to use figures, tables, graphs, etc. in subsequent publications using files prepared and formatted by you or the APS-prepared versions. The appropriate bibliographic citation must be included.
- **As the author of an APS-published article, may I include my article or a portion of my article in my thesis or dissertation?** Yes, the author has the right to use the article or a portion of the article in a thesis or dissertation without requesting permission from APS, provided the bibliographic citation and the APS copyright credit line are given on the appropriate pages.

Vita

Argenis Daniel Da Silva was born in Cumaná, Venezuela. He received the *Licenciatura en Física* degree from Universidad de Oriente (Venezuela) in 1999.